S. K. Nechaev, O. A. Vasil'ev, On the Metric Structure of Ultrametric Spaces, *Труды МИАН*, 2004, том 245, 182–201

ТРУДЫ МАТЕМАТИЧЕСКОГО ИНСТИТУТА ИМ. В.А. СТЕКЛОВА, 2004, т. 245, с. 182–201

УДК 517.94+512.625

On the Metric Structure of Ultrametric Spaces

©2004 г. S. K. Nechaev[1], O. A. Vasilyev[2]

Поступило в ноябре 2003 г.

In our work, we reconsider the old problem of diffusion at the boundary of an ultrametric tree from a "number-theoretic" point of view. Namely, we use modular functions (in particular, the Dedekind η function) to construct a "continuous" analogue of the Cayley tree isometrically embedded into the Poincaré upper half-plane. Later, we work with this continuous Cayley tree as with a standard function of a complex variable. In the frameworks of our approach, the results of Ogielsky and Stein on the dynamics on ultrametric spaces are reproduced semi-analytically/semi-numerically. Speculation on the new "geometrical" interpretation of the replica $n \to 0$ limit is proposed.

1. INTRODUCTION

Let us begin with an obvious and almost tautological statement: any regular tree has an ultrametric structure. Recall that the ultrametricity of the space $\mathcal{H}$ implies the strong triangle inequality, which means that the distances r_{AB}, r_{BC}, and r_{AC} between any three points A, B, and C in the space $\mathcal{H}$ satisfy the condition $r_{AC} \leq \max\{r_{AB}, r_{BC}\}$ (see, for example, [1]). Having appeared in mathematical literature in connection with p-adic analysis (see [2, 3] for a review), ultrametric spaces became very popular in physical community because of their importance for spin glasses (for a review, see [4] and references therein).

The famous replica symmetry breaking (RSB) scheme [5–8] is ultimately connected with the ultrametric structure of the phase space of many disordered systems exhibiting the spin-glass behavior. Since the invention of the RSB, many authors, both physicists and mathematicians, have attempted to adapt p-adic analysis for physical needs, mainly trying to elucidate and justify the replica $n \to 0$ limit. However, from our point of view, the interpretation of spin-glass problems in terms of p-adic language does not converge well. As an exception, one has to mention recent interesting contributions to that subject [9–11], where the application of the p-adic Fourier transform allows one to significantly simplify the solution to the problem of diffusion on an ultrametric tree. One can hope that the continuation and generalization of these works would allow deeper penetration of p-adic analysis into the physics of disordered systems with ultrametric phase spaces, such as spin glasses, neural networks, and disordered heteropolymers (see [11, 12] for the detailed list of relevant references).

In what follows, we will always keep in mind the $(p+1)$-branching Cayley tree as an example of an ultrametric space. Despite extremely simple topological structure of a tree, one cannot operate in this space as in a usual space with a Euclidean metric because the number of degrees of freedom for the $(p+1)$-branching Cayley tree grows exponentially with the size of the tree. For some problems, such as the branching process on Cayley trees and treelike graphs, it is not sufficient to deal only with the "distance" measured in the number of generations between two points on the graph, but it is ultimately necessary to know the absolute values of the coordinates of points on the Cayley tree. The main difficulty concerns the encoding of the Cayley tree vertices. This problem becomes very cumbersome because, for a tree, we do not have any transparent and convenient "coordinate system,"

[1]LPTMS, Université Paris Sud, 91405 Orsay Cedex, France; Институт теоретической физики им. Л.Д. Ландау РАН, Москва, Россия.
E-mail: nechaev@landau.ac.ru

[2]Институт теоретической физики им. Л.Д. Ландау РАН, Москва, Россия.

like a D-dimensional grid in a D-dimensional Euclidean space. One of possible ways to resolve the addressed problem consists in using p-adic analysis [13, 14]. The vertices of the graph $\mathcal{C}$, i.e., of the $(p+1)$-branching Cayley tree, admit natural parameterizations by p-adic numbers, which enables one to develop the whole machinery like a p-adic Fourier transform, etc. This way was exploited in [9–11].

Another possibility, described in the present paper, consists in the following. Instead of working with the ultrametric discrete graph $\mathcal{C}$, one can embed this graph into the metric space $\mathcal{H}$ preserving all ultrametric properties of $\mathcal{C}$. Note that any image of a regular Cayley tree refers indirectly to the isometric embedding of a tree into the complex plane. Indeed, a Cayley tree is usually drawn in such a way that any new generation of vertices (counted from the root point) is smaller than the previous generation in geometric progression. Taking advantage of the isometric embedding, one can

- naturally parameterize the vertices of the Cayley graph $\mathcal{C}$ by an ordinary complex variable $z = x + iy$ in the complex plane z without using any ingredients of p-adic analysis;
- construct a continuous analogue of a Cayley tree, i.e., a continuous space $\mathcal{H}$ with ultrametric properties borrowed from the initial Cayley tree.

The paper is organized as follows. In Sections 2–6, we describe the way of isometric embedding of a regular 3-branching Cayley tree $\mathcal{C}$ into the complex upper half-plane $z = x + iy$ and discuss the ultrametric properties of the resulting space $\mathcal{H}$. The problem of diffusion on the boundary of an ultrametric tree $\mathcal{C}$ embedded into the space $\mathcal{H}$ is considered in Section 7. The results are summarized in the conclusion, where we also express some conjectures concerning the possible geometrical interpretation of the replica $n \to 0$ limit.

2. CONTINUOUS ANALOGUE OF AN ISOMETRIC CAYLEY TREE

It is well known that any regular Cayley tree, as an exponentially growing structure, cannot be isometrically embedded into a Euclidean plane. Recall that the embedding of a Cayley tree $\mathcal{C}$ into a metric space is called *isometric* if $\mathcal{C}$ covers this space, preserving all angles and distances. For example, a rectangular lattice isometrically covers the Euclidean plane $\mathcal{E} = \{x, y\}$ with the flat metric $ds^2 = dx^2 + dy^2$. In the same way, the Cayley tree $\mathcal{C}$ isometrically covers the surface of constant negative curvature (the Lobachevsky plane) $\mathcal{H}$. One of possible representations of $\mathcal{H}$, known as a Poincaré model, is the upper half-plane $\operatorname{Im} z > 0$ of the complex plane $z = x + iy$ endowed with the metric $ds^2 = \frac{dx^2+dy^2}{y^2}$ of constant negative curvature.

This and the following sections are aimed at constructing a "continuous" analogue of the standard 3-branching Cayley tree by means of modular functions and analyzing the structure of the barriers separating the neighboring valleys. Due to the specific number-theoretic properties of modular functions, these barriers are ultrametrically organized.

To be precise, let us begin with the explicit description of the standard recursive construction that allows the encoding of all vertices of the 3-branching Cayley tree $\mathcal{C}$ isometrically covering the surface of constant negative curvature $\mathcal{H} = \{z|\ \operatorname{Im} z > 0\}$. Recall that the 3-branching Cayley tree is the Cayley graph of the group Λ that has a free product structure: $\Lambda \sim \mathbb{Z}_2 \otimes \mathbb{Z}_2 \otimes \mathbb{Z}_2$ (where $\mathbb{Z}_2$ is the cyclic group of the second order). The matrix representation of the generators h_1, h_2, and h_3 of the group Λ is well known (see, for example, [15]):

$$h_1 = \begin{pmatrix} 1 & -\frac{2}{\sqrt{3}} \\ 0 & -1 \end{pmatrix}, \qquad h_2 = \begin{pmatrix} 1 & \frac{2}{\sqrt{3}} \\ 0 & -1 \end{pmatrix}, \qquad h_3 = \begin{pmatrix} 0 & \frac{1}{\sqrt{3}} \\ \sqrt{3} & 0 \end{pmatrix}. \tag{1}$$

For our purposes, it is convenient to take a framing consisting of the composition of the standard fractional-linear transform and the complex conjugacy. Namely, denoting by $\overline{z}$ the complex

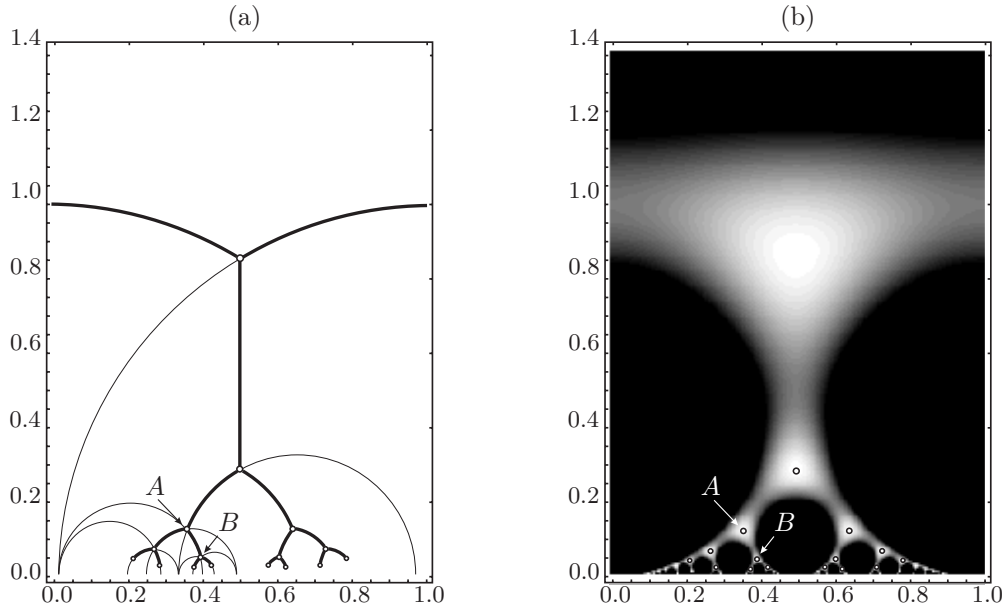

Fig. 1. (a) The 3-branching Cayley tree isometrically embedded into the Poincaré hyperbolic upper half-plane $\mathcal{H}$. (b) The density plot of the function $f(z)$ (see the text) in the rectangle $\{0 \le \operatorname{Re} z \le 1,\ 0.01 \le \operatorname{Im} z \le 1.4\}$

conjugate of z, we consider the following action in $\mathcal{H}$:

$$\begin{pmatrix} a & b \\ c & d \end{pmatrix} : \ z \to \frac{a\overline{z}+b}{c\overline{z}+d}. \tag{2}$$

We raise the Cayley tree $\mathcal{C}$ in $\mathcal{H}$ as follows. Take the set of generators $\{h_1, h_2, h_3\}$ of the group Λ. Choose the point $(x_0, iy_0) = (0, i)$ as the root of the tree.

Any vertex in the generation n from the root point of the tree $\mathcal{C}$ is associated with an element $M_n = \prod_{k=1}^{n} h_{\alpha_k}$ of the group Λ (where $\alpha_k \in \{1, 2, 3\}$ for any k). All vertices are parameterized by the complex coordinates $z_n = M_n\big((-1)^n\, i\big)$ in $\mathcal{H}$. For example, the coordinates of the points z_A and z_B in Fig. 1 can be obtained in the following way. Multiply the generators h_i along the trajectory in the inverse order, i.e., *from* the points z_A and z_B *to* the root point i. Then, we arrive at

$$M_2^{(A)} \equiv \begin{pmatrix} a & b \\ c & d \end{pmatrix} = h_3\, h_2 = \begin{pmatrix} 0 & \frac{1}{\sqrt{3}} \\ \sqrt{3} & 0 \end{pmatrix} \begin{pmatrix} 1 & \frac{2}{\sqrt{3}} \\ 0 & -1 \end{pmatrix} = \begin{pmatrix} 0 & -\frac{1}{\sqrt{3}} \\ \sqrt{3} & 2 \end{pmatrix},$$

$$M_3^{(B)} \equiv \begin{pmatrix} a & b \\ c & d \end{pmatrix} = h_3\, h_2\, h_3 = \begin{pmatrix} 0 & \frac{1}{\sqrt{3}} \\ \sqrt{3} & 0 \end{pmatrix} \begin{pmatrix} 1 & \frac{2}{\sqrt{3}} \\ 0 & -1 \end{pmatrix} \begin{pmatrix} 0 & \frac{1}{\sqrt{3}} \\ \sqrt{3} & 0 \end{pmatrix} = \begin{pmatrix} -1 & 0 \\ 2\sqrt{3} & 1 \end{pmatrix}.$$

Using (2) and the matrices $M_2^{(A)}$ and $M_3^{(B)}$, we get

$$z_A = \frac{0 \times i - \frac{1}{\sqrt{3}}}{\sqrt{3} \times i + 2} = -\frac{2}{7\sqrt{3}} + \frac{i}{7},$$

$$z_B = \frac{(-1) \times (-i) + 0}{2\sqrt{3} \times (-i) + 1} = -\frac{2\sqrt{3}}{13} + \frac{i}{13}.$$

To establish a connection with the forthcoming constructions, we will make a simple linear transform of z: $z \to \frac{\sqrt{3}}{2} z + \frac{1}{2}$. The coordinates of the points A and B after such a transform are shown in Fig. 1.

However, from our point of view, such a recursive construction has a crucial drawback: one cannot automatically encode all vertices of the tree introducing a sort of a coordinate system as, say, in the Euclidean plane. Actually, we know that any vertex of a rectangular grid in the Euclidean plane has coordinates (am, bn), where $\{m, n\} \in \mathbb{Z}$ and (a, b) are the length and the width of the elementary cell of the lattice. Our desire is to construct a somewhat similar system for homogeneous trees. More specifically, we aim at finding an analytic function $f(z)$ defined in $\operatorname{Im} z > 0$ all of whose zeros give all coordinates of the vertices of the 3-branching homogeneous Cayley tree $\mathcal{C}$ isometrically embedded into $\mathcal{H}(z \mid \operatorname{Im} z > 0)$. Below, we describe the construction of the corresponding function $f(z \mid \operatorname{Im} z > 0)$ and discuss its properties in connection with the geometry of ultrametric spaces. The forthcoming construction is based on the properties of the Dedekind η function. Recall the standard definition of the function $\eta(z)$ (see, for instance, [16]):

$$\eta(z) = e^{\pi i z/12} \prod_{k=0}^{\infty} (1 - e^{2\pi i k z}), \qquad \operatorname{Im} z > 0. \tag{3}$$

It is well known [16] that the Dedekind η function is connected with the elliptic Jacobi ϑ functions by the following relation:

$$\vartheta_1'(0, e^{\pi i z}) = \eta^3(z), \tag{4}$$

where

$$\vartheta_1'(0, e^{\pi i z}) \equiv \left.\frac{d\vartheta_1(u, e^{\pi i z})}{du}\right|_{u=0} = 2e^{\pi i z/4} \sum_{n=0}^{\infty} (-1)^n (2n+1) e^{\pi i n(n+1) z}. \tag{5}$$

Now, we can formulate the central assertion of the paper. Define the function $f(z)$ as follows:

$$f(z) = C^{-1} \, |\eta(z)| \, (\operatorname{Im} z)^{1/4}, \tag{6}$$

where C is a normalization constant,

$$C = \left|\eta\left(\frac{1}{2} + i\frac{\sqrt{3}}{2}\right)\right| \left(\frac{\sqrt{3}}{2}\right)^{1/4} = 0.772\,301\,84\ldots . \tag{7}$$

The normalization constant C is chosen to set the maximal value of the function $f(z)$ to 1: $0 < f(z) \le 1$ for any z in the upper half-plane $\operatorname{Im} z > 0$. It can be proved that the function $f(z)$ has the following remarkable properties:

1. The function $f(z) - 1$ has zeros at the points z_{cen} (and only at these points), the centers of zero-angled triangles tesselating the Poincaré hyperbolic upper half-plane $\mathcal{H}(z \mid \operatorname{Im} z > 0)$.
2. The function $f(z)$ has local maxima at all the points z_{cen} and only at these points.

All the solutions of the equation $f(z) - 1 = 0$ define all the coordinates of the 3-branching Cayley tree isometrically embedded into the upper half-plane $\mathcal{H}(z \mid \operatorname{Im} z > 0)$. The corresponding density plot of the function $f(z)$ in the region $\{0 \le \operatorname{Re} z \le 1,\ 0.04 \le \operatorname{Im} z \le 1.4\}$ is shown in Fig. 2. It is noteworthy that the function $Z(z) = [Cf(z)]^{-2}$ is the partition function of a free bosonic field on a torus [17]. The function $Z(z)$ has been extensively studied in the conformal field theory. In particular, it can easily be verified that the function $Z(z)$ is invariant with respect to the action of the modular group $PSL(2, \mathbb{Z})$, namely,

$$\begin{cases} Z(z) = Z(z+1), \\ Z(z) = Z\left(-\dfrac{1}{z}\right). \end{cases} \tag{8}$$

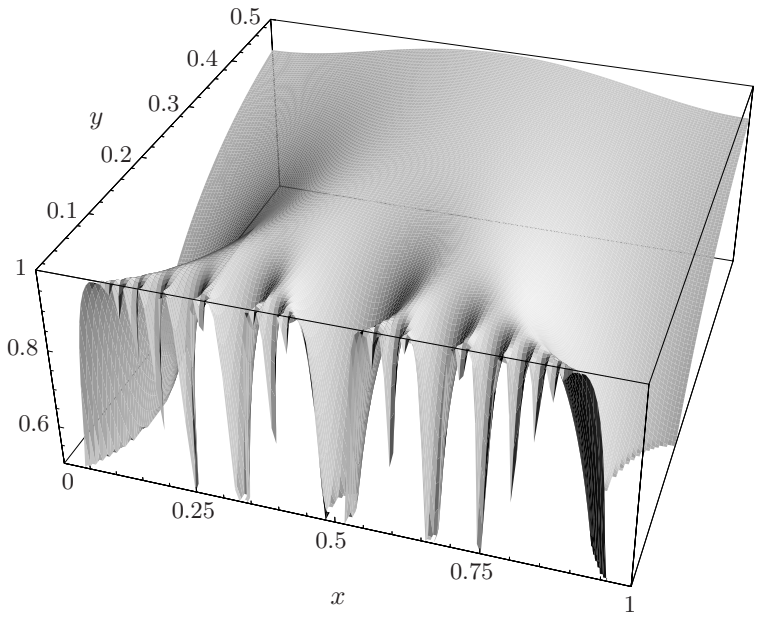

Fig. 2. Relief of the function $f(z)$ in the rectangle $\{0 \le \operatorname{Re} z \le 1,\ 0.04 \le \operatorname{Im} z \le 1.4\}$

Later on, we will address to these self-dual properties. The proof of properties 1 and 2 of the function $f(z)$ implies verifying that the function $f(z)$ is invariant with respect to the conformal transform $z^{(1)}(z)$ of the Poincaré half-plane to itself

$$z^{(1)}(z) = \frac{z - z_0}{z\overline{z}_0 - 1}, \tag{9}$$

where z_0 is the coordinate of any center of a zero-angled triangle in the hyperbolic Poincaré upper half-plane obtained from the initial one by successive transformations. Hence, it is necessary and sufficient to show that the values of the function $f(z)$ at the nearest centers of circular triangles are equal and reach the maximal value 1:

$$f\left(z = \frac{1}{2} + i\frac{\sqrt{3}}{2}\right) = f\left(z = \pm 1 + \frac{1}{2} + i\frac{\sqrt{3}}{2}\right) = f\left(z = \frac{1}{2} + i\frac{\sqrt{3}}{6}\right) = 1. \tag{10}$$

Then, taking $z_0 = \left\{\left(\frac{3}{2} + i\frac{\sqrt{3}}{2}\right); \left(-\frac{1}{2} + i\frac{\sqrt{3}}{2}\right); \left(\frac{1}{2} + i\frac{\sqrt{3}}{6}\right)\right\}$ and performing the conformal transform (9), we move the centers of the first generation of zero-angled triangles to the new centers (second generation) located at $z^{(1)}$. Now, we can repeat recursively the construction, i.e., find the new coordinates of the centers of the third generation of zero-angled triangles, $z^{(2)}(z^{(1)})$, and compute the function $f(z)$ at these points; then, we perform the conformal transform $z^{(3)}(z^{(2)})$, and so on. Let us use now the following well-known properties of the Jacobi elliptic ϑ functions [16]:

$$\eta\left(\frac{pz + r}{qz + s}\right) = \omega\sqrt{rz + s}\,\eta(z), \tag{11}$$

where $\operatorname{Im} z > 0$, $\{p, q, r, s\} \in \mathbb{Z}$, $ps - qr = 1$, and ω is some 24th-power root of unity that depends on the coefficients p, q, r, and s but does not depend on z. Using (11), we can write

$$\begin{cases} \eta(z + k) = \eta(z), & k = \pm 1, \pm 2, \pm 3, \dots, \\ \eta\left(\dfrac{1}{2} + \dfrac{i}{2\sqrt{\lambda}}\right)\lambda^{-1/4} = \eta\left(\dfrac{1}{2} + \dfrac{i\sqrt{\lambda}}{2}\right), & \lambda > 0. \end{cases} \tag{12}$$

Now, we can easily check relations (10). In turn, (8) can be regarded as a particular case of (11). The fact that the function $f(z)$ has local maxima at the points z_{cen} can be verified straightforwardly by differentiating $f(z)$ with respect to z at the points z_{cen}. The 3D relief of the function $f(z)$ is shown in Fig. 2. One can clearly see a treelike structure of hills separated by valleys.

Let us note an important duality relation for the Dedekind function that is established by the mapping $y \leftrightarrow \frac{1}{y}$ (where $y = \operatorname{Im} z$, $y > 0$). For all $\{p, q, r, s\} \in \mathbb{Z}$ such that $ps - qr = 1$, the following equation is satisfied:

$$\left|\eta\left(\left\{\frac{p}{q}\right\} + iy\right)\right| = \left|\eta\left(\left\{\frac{s}{q}\right\} + \frac{i}{q^2 y}\right)\right| \frac{1}{\sqrt{qy}}, \tag{13}$$

where $\left\{\frac{p}{q}\right\}$ and $\left\{\frac{s}{q}\right\}$ denote the fractional parts of the corresponding quotients. Relation (13) will be used in the forthcoming sections for practical purposes of numerical computation. In the next section, we discuss the ultrametric organization of corresponding barriers. We regard the 3D relief constructed on the basis of the function $f(z)$ (see Fig. 2) as a continuous analogue of the Cayley tree isometrically embedded into $\mathcal{H}(z \mid \operatorname{Im} z > 0)$.

3. ULTRAMETRIC STRUCTURE OF BARRIERS IN THE STANDARD RSB SCHEME AND IN THE TREELIKE METRIC SPACE

The replica symmetric breaking (RSB) scheme [5–8] has appeared in the spin-glass theory as a self-consistent approach that is free of many drawbacks of the replica symmetric consideration. Later on, it was realized that the RSB structure naturally appears in the problem of diffusion on the boundary of a Cayley tree [18, 19], where the neighboring sites are separated by barriers that are hierarchically organized according to their ultrametric distances on the Cayley tree. For example, the neighboring points A, B and B, C at the boundary of the 3-branching Cayley tree (see Fig. 3) are separated by barriers depending on the ultrametric distances between the points A, B and B, C on the tree.

Recall that two points, say, B and C in Fig. 3, are separated by a potential barrier depending on the number of the Cayley tree generations from the points B and C to their common parent branch. Let us label the states at the Lth generation of the 3-branching Cayley tree by an integer k ($1 \le k \le 2^L$). If we represent k by a binary sequence, then the ultrametric distance between the

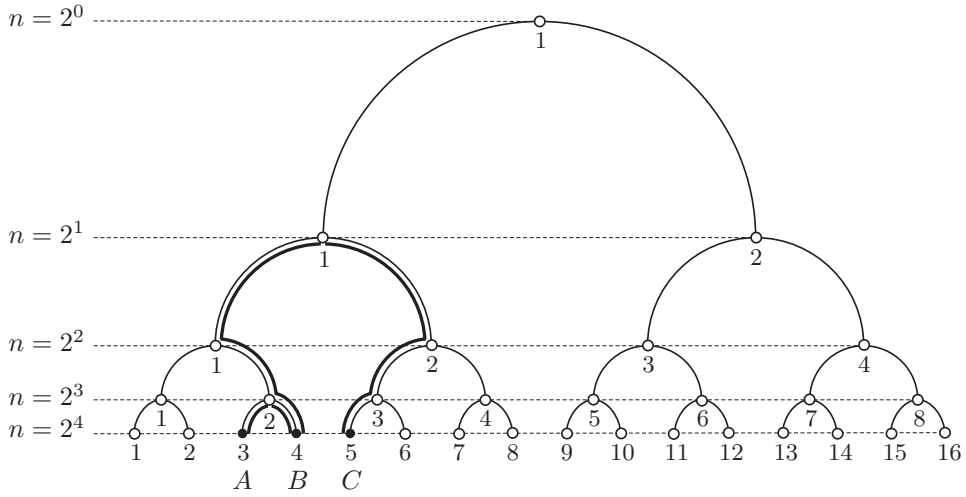

Fig. 3. The 3-branching Cayley tree. The ultrametric distances between the points A, B and B, C are shown by heavy lines; n is the number of states in each generation of the tree, the maximal number of generations being $L = 4$

points B and C will coincide with the highest distinct rank in the binary expressions of $k_B = 4$ and $k_C = 5$.

Denote by q_m the Boltzmann weights at the boundary of a 3-branching Cayley tree associated with the barriers of ultrametric height m. All the barriers can be encoded in the $2^L \times 2^L$ RSB matrix $\mathbf{Q}(q_0, q_1, \ldots, q_L)$ having the structure shown in (14) for $L = 3$. Keeping in mind the relation to spin glasses, we associate the total number of states 2^L with the total number of replicas n in the standard RSB scheme.

$$\mathbf{Q} = \left[\begin{array}{cccc|cccc} q_0 & q_1 & q_2 & q_2 & q_3 & q_3 & q_3 & q_3 \\ q_1 & q_0 & q_2 & q_2 & q_3 & q_3 & q_3 & q_3 \\ \hline q_2 & q_2 & q_0 & q_1 & q_3 & q_3 & q_3 & q_3 \\ q_2 & q_2 & q_1 & q_0 & q_3 & q_3 & q_3 & q_3 \\ \hline q_3 & q_3 & q_3 & q_3 & q_0 & q_1 & q_2 & q_2 \\ q_3 & q_3 & q_3 & q_3 & q_1 & q_0 & q_2 & q_2 \\ \hline q_3 & q_3 & q_3 & q_3 & q_2 & q_2 & q_0 & q_1 \\ q_3 & q_3 & q_3 & q_3 & q_2 & q_2 & q_1 & q_0 \end{array}\right] \tag{14}$$

The values $p_m = \frac{1}{n} q_m$ $(m = 1, \ldots, L)$ define the jumping probabilities from some vertex k_1 to another vertex k_2 at the boundary of a 3-branching Cayley tree separated by a barrier of ultrametric height m, while the value p_0 is assigned to the probability to stay at a given vertex. In each row of the matrix $\mathbf{Q}$, the sum of probabilities is equal to 1. In most physically important situations, the Boltzmann weights q_m depend on m either exponentially or polynomially:

$$q_m = \begin{cases} \text{const} \cdot m^{\alpha}, \\ \text{const} \cdot e^{-\beta m}. \end{cases} \tag{15}$$

Later on, we pay attention only to the exponential dependence of q_m on m, i.e., to the case when $q_m = \text{const} \cdot e^{-\beta m}$ (where β stands for the inverse temperature). The probability p_0 to stay at a given vertex can be explicitly computed from the conservation condition $\sum_{m=0}^{n} P_m = 1$, and for $q_m = \text{const} \cdot e^{-\beta m}$, it reads

$$p_0 = 1 - \frac{1}{n} \sum_{j=1}^{L} 2^j \, e^{-\beta j} = 1 - \frac{2(1 - 2^L e^{-\beta L})}{n(2 - e^{\beta})}. \tag{16}$$

In order to understand the connection between the ultrametric structure of the barriers in the case of a 3-branching Cayley tree and its continuous analogue isometrically embedded into $\mathcal{H}(z \mid \operatorname{Im} z > 0)$, let us begin with the following observation. We can consider the function $v(x|y) = -\ln f(x|y)$ (where $x = \operatorname{Re} z$) as the potential relief at the boundary of the Cayley tree cut at the distance $y = \operatorname{Im} z$ from the real axis. The typical shapes of the function $v(x|y)$ for a few fixed values 0.04, 0.008, and 0.0016 of y are shown in Fig. 4. This picture clearly demonstrates the ultrametric organization of the barriers that separate the valleys.

Figure 4 shows that the distance from the real axis y characterizes the number of the Cayley tree generations: the smaller the value of y is, the greater the number of new generations of barriers that appear (and the higher the barriers are). The relation of the system of barriers shown in Fig. 4 to the structure of the RSB matrix (14) becomes now very obvious. The barriers of the smallest scale correspond to the values q_1 in the matrix $\mathbf{Q}(q_0, q_1, \ldots, q_L)$, the barriers of the next scale correspond to q_2, etc. Hence, the distance y can be considered as a parameter that controls the size of the RSB matrix: as $y \to 0$, the size of $\mathbf{Q}$ tends to infinity. Thus, one can conjecture that the number of the replicas n is a function of y.

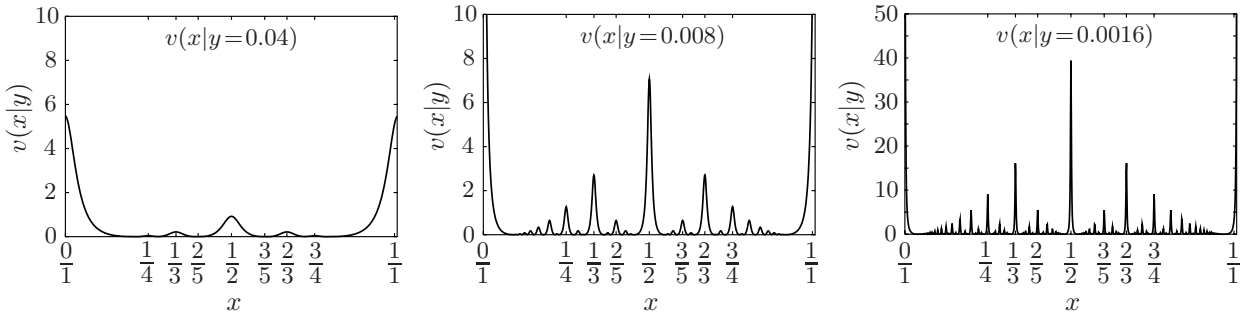

Fig. 4. Typical shape of the function $v(x|y) = -\ln f(x)$ for $y = 0.04,\ 0.008,\ 0.0016$

This relation will be discussed at length in Section 7. The function $v(x) = -\ln f(x)$, defined on the interval $0 < x < 1$, has the properties borrowed from the structure of the underlying modular group $PSL(2,\mathbb{Z})$ acting in the half-plane $\mathcal{H}(z \,|\, y > 0)$ [20, 21]. In particular,

- the local maxima of the function $v(x)$ are located at rational points;
- the highest barrier on a given interval $\Delta x = [x_1, x_2]$ is located at a rational point $\frac{p}{q}$ with the smallest denominator q. On a given interval $\Delta x = [x_1, x_2]$, there is only one such point. The locations of the barriers with successive heights on the interval Δx are arranged according to the group operation

$$\frac{p_1}{q_1} \oplus \frac{p_2}{q_2} = \frac{p_1 + p_2}{q_1 + q_2}. \tag{17}$$

Figure 4 clarifies this statement. The highest barriers on the interval $0 \le x \le 1$ are located at the points $x_0 = 0$ and $x_1 = 1$. Rewriting 0 and 1 as $\frac{0}{1}$ and $\frac{1}{1}$, respectively, we can find the location point x_2 of the barrier with the next maximal height. Namely, $x_2 = \frac{0}{1} \oplus \frac{1}{1} = \frac{0+1}{1+1} = \frac{1}{2}$. Continuing this construction, we arrive at a hierarchical structure of barriers located at rational points organized in the Farey sequence. According to our construction, this should replace the standard RSB scheme. The corresponding modular (MRSB) matrix will be constructed in the next section.

4. EXPLICIT ORGANIZATION OF BARRIERS ON THE BASIS OF THE DEDEKIND FUNCTION

The aforesaid gives us the idea of the construction. However, to establish the precise connection between the standard RSB scheme and the number-theoretic MRSB scheme, we should construct the MRSB scheme with the exponential organization of the Boltzmann weights, as in the RSB. Recall that the ultrametric distance between two points A and B on the Cayley graph is equal to half the number of steps of the shortest path connecting these points. For example, the ultrametric distances r_{AB} (between the points A and B) and r_{AC} (between the points A and C) in Fig. 3 are as follows: $r_{AB} = 1$ and $r_{AC} = 3$. It is clearly seen that the points A and C (as well as the points B and C) are separated by the barrier located at the point $x_1 = \frac{1}{3}$, while the points A and B are separated by the barrier located at the point $x_2 = \frac{2}{7}$. According to the last equation in (15), the height U_m of the barrier between two points separated by the ultrametric distance m in the standard RSB scheme reads

$$U_m^{\mathrm{RSB}} \equiv -\ln q_m = \beta m. \tag{18}$$

The dependence of the Boltzmann weights on the ultrametric distance in the MRSB scheme should also satisfy (18). This implies that the heights U^{MRSB} of the MRSB barriers should linearly depend on the ultrametric distance between two vertices of the Cayley tree. To adjust the heights of the

barriers in the MRSB and RSB schemes, some auxiliary work has to be done. The corresponding construction is described in the rest of this section. Begin with the standard RSB tree and distribute the barriers separating all 2^L boundary points of the Cayley tree in the generation L equidistantly over the unit interval $[0,1]$. For example, for $L=1$, there are two vertices of the Cayley tree separated by a single barrier located at the point $x_1=\frac{1}{2}$. The barriers of the second generation $L=2$ are situated at the points $x_2^{(1)}=\frac{1}{4}$ and $x_2^{(2)}=\frac{3}{4}$. For $L=3$, we have $x_3^{(1)}=\frac{1}{8}$, $x_3^{(2)}=\frac{3}{8}$, $x_3^{(3)}=\frac{5}{8}$, $x_3^{(4)}=\frac{7}{8}$, etc. The points $x_L^{(j)}=\frac{j}{2^L}$ (where j is odd and $1<j<2^L$) are uniformly distributed over the unit interval $[0,1]$. Let us normalize the barrier heights as follows. In a finite Cayley tree of L generations, there are 2^{L-1} *smallest* barriers; all of them have the same height. Require these barriers to be of height $U(L)=\frac{1}{L}$. Then, the *averaged* barriers in some intermediate generation m $(1\le m\le L)$ have the height

$$U(m,L)=\frac{L-m+1}{L}\equiv 1-\frac{m-1}{L}. \tag{19}$$

Hence, in the first generation $m=1$, the height of a single barrier located at the point $x_1=\frac{1}{2}$ is normalized by 1: $U(m=1,L)=1$. This sets our normalization condition. Let us note that a choice of the normalization of the barriers can be considered as the renormalization of the inverse temperature $\beta\to\widetilde{\beta}L$ (see (18)). The physical sense of such renormalization consists in the following. When the number L of Cayley tree generations is increased, the corresponding landscape acquires more and more small-scale details without changing the height of the maximal barrier, which is always normalized by 1.

Now, we apply a similar procedure to the continuous MRSB structure. Recall that the logarithm of the Dedekind function has maxima at rational points $x=\frac{p}{q}$. The set of these points $\{x_i\}$ can be generated recursively, as it was explained above in connection with equation (17). We start with two "parent" points $0=\frac{0}{1}$ and $1=\frac{1}{1}$ of the zeroth generation. At the first step, we generate a barrier at the point $\frac{1}{2}=\frac{0+1}{1+1}$; at the second step, we generate two barriers at the points $\frac{1}{3}=\frac{0+1}{1+2}$ and $\frac{2}{3}=\frac{1+1}{2+1}$, and so on. The number of recursive steps necessary to arrive at a barrier located at a specific point $x=\frac{p}{q}$ is called the *generation* in which this barrier has appeared for the first time.

Let us fix the maximal generation L. Denote by $\{x_i\}(m)$ the set of points in the generation $m\le L$ at which the barriers are located. There are 2^{m-1} such points. For example, $\{x_i\}(m=1)=\{\frac{1}{2}\}$, $\{x_i\}(m=2)=\{\frac{1}{3},\frac{2}{3}\}$, $\{x_i\}(m=3)=\{\frac{1}{4},\frac{2}{5},\frac{3}{5},\frac{3}{4}\}$, and so on. Now, we need to express the heights $U^{\mathrm{MRSB}}(x_i,m,y)$ of the barriers up to the generation $m\le L$ in terms of the Dedekind function $\eta(x_i,y)$. Take the logarithm of the normalized Dedekind function

$$h(x,y)=-\ln f(x,y) \tag{20}$$

as a possible basis for such a construction (the function $f(x,y)$ is defined in (6)). Our choice is justified by the fact that this function has maxima at the points $\{x_i\}(m)$ and exhibits ultrametric behavior. Starting from $m\ge 3$, the values of the function $h(x_i,m,y)$ at the points of maxima $\{x_i\}(m)$ become unequal. In Fig. 5a, we plot the minimal $h_{\min}(m,y)=\min(h(x_i,m,y))$, the average $h_{\mathrm{avr}}(m,y)=\langle h(x_i,m,y)\rangle$, and the maximal $h_{\max}(m,y)=\max(h(x_i,m,y))$ barrier heights in each of the three generations $m=4,6,8$. The brackets $\langle\ldots\rangle$ denote the averaging over all barriers in the generation m. The function $0.001\,y^{-1}$ is plotted for comparison in the same figure.

Figure 5a allows us to conclude that $h(m,y)\sim y^{-1}$ for fixed m. More detailed information about the function $h_{\mathrm{avr}}(m,y)=\langle-\ln f(x_i,y)\rangle$ can be extracted from Fig. 5b, which is similar to Fig. 5a but is extended up to $m\in[1,10]$. The data shown in Fig. 5b are approximated by the natural fit

$$h_{\mathrm{avr}}=a_m y^{b_m}$$

Table 1. Numerical results of the fit $h_{\rm avr} = a_m y^{b_m}$

m	a_m	b_m	m	a_m	b_m
1	0.0594(8)	−1.008(2)	6	0.000 84(7)	−1.04(1)
2	0.0263(4)	−1.008(1)	7	0.000 31(4)	−1.06(1)
3	0.0118(2)	−1.011(1)	8	0.000 118(17)	−1.08(6)
4	0.0053(1)	−1.014(2)	9	0.000 040(7)	−1.102(1)
5	0.002 30(7)	−1.021(3)	10	0.000 012(3)	−1.14(2)

for all points such that $h_{\rm avr} > 10$. The results of our approximation are shown in Table 1, as well as are drawn in Fig. 5b by lines.

The coefficient a_m is plotted as a function of m in Fig. 6a. The approximation $a_m \simeq 0.144(8)\, e^{-0.847(18)\, m}$ is shown in the same figure by the dashed line. Hence, we expect the following relation: $h(m, y) \simeq 0.144(8)\, e^{-0.847(18)\, m}\, y^{-1}$.

The analysis of the numerical data for the averaged logarithm of the Dedekind function allows us to conjecture the general ansatz

$$h_{\rm avr}(m, y) \equiv \langle -\ln f(x_i, y)\rangle = d(y)\, e^{-c(y)\, m}\, y^{-1}. \tag{21}$$

This equation establishes functional dependence of the average height $h_{\rm avr}$ on the generation m ($m = 1, 2, \dots$) for fixed y. Recall that the generation m is defined as the minimal number of recursive steps necessary to arrive at a barrier located at a specific point $x_i = \frac{p}{q}$. Let us fix now the maximal generation L. Our desire is to obtain the normalized barrier for the MRSB scheme like it has been done for the RSB (see (19)). Taking into account that (21) is valid for any $m \geq 1$, we can extract m from (21) and write it as follows:

$$m = 1 + \frac{1}{c(y)} \ln \frac{h_{\rm avr}(m, y)}{h_{\rm avr}(m = 1, y)}. \tag{22}$$

Substituting (22) into (19), we get the following formal expression for the height of the barriers in the MRSB scheme:

$$U^{\rm MRSB}(x_m, y, L) \equiv 1 - \frac{m-1}{L} = 1 + \frac{1}{c(y)\, L} \ln \frac{h_{\rm avr}(m, y)}{h_{\rm avr}(1, y)}. \tag{23}$$

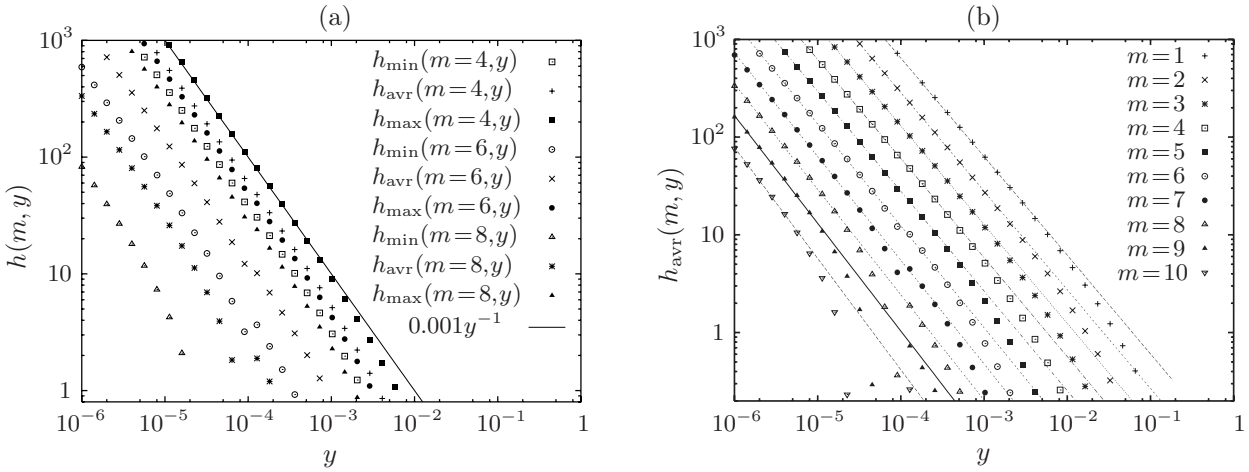

Fig. 5. (a) Minimal $h_{\rm min}(y)$, average $h_{\rm avr}(y)$, and maximal $h_{\rm max}(y)$ barriers for $m = 4, 6, 8$. (b) The function $h_{\rm avr}(y)$ for $m = 1, \dots, 10$

Table 2. Dependence of the parameter $c(y)$ on $y = y^*$ up to $L = 10$ generations (see (25))

y^*	$c(y^*)$	y^*	$c(y^*)$	y^*	$c(y^*)$
5.12×10^{-5}	0.820(11)	3.2×10^{-6}	0.7623(22)	4×10^{-7}	0.7544(32)
2.56×10^{-5}	0.8057(99)	1.6×10^{-6}	0.7579(27)	2×10^{-7}	0.7538(37)
1.28×10^{-5}	0.7944(86)	8×10^{-7}	0.7556(30)	1×10^{-7}	0.7535(34)
6.4×10^{-6}	0.7718(29)				

Now, we should explain how one can apply the formal equation (23) to practical computations. Let us fix the maximal generation L and define the value y^* from the equation

$$h_{\rm avr}(L, y^*) = 1. \tag{24}$$

The value y^* has the following sense. For all $y < y^*$, the value $h_{\rm avr}(m, y)$ does not depend on m ($m \le L$) because all barriers in the generation m are already presented, and hence, the average height $h_{\rm avr}$ cannot be changed for any $y < y^*$. Therefore, we can postulate that, for all $y < y^*$, the height of the barrier is described by the function

$$U^{\rm MRSB}(x_i) = 1 + \frac{1}{c(y^*)\,L} \ln \frac{\ln f(x_i, y^*)}{\ln f\left(\frac{1}{2}, y^*\right)}, \tag{25}$$

where x_i is the rational point of the barrier location and we have used (20). The discussion of the dependence $c(y^*)$ deserves special attention. As is shown in Table 2, for sufficiently small y^*, the value of c tends to a constant. Thus, the function $U^{\rm MRSB}(x_i)$ defines the heights of ultrametric barriers in the MRSB scheme that are fully consistent with the heights of the RSB barriers for the Cayley tree. It should be noted that, for intermediate values of y, some barriers of large generations are negative due to the cut (24); however, having m, we can always find y^* such that all barriers are positive. For example, for $y \le y^* = 10^{-6}$, all barriers up to $m = 10$ generations are positive.

Our tedious but simple construction is clearly illustrated in Fig. 7, where we plot the heights of barriers $U^{\rm MRSB}(x_i)$ at rational points x_i up to the generation $L = 10$ for $y^* = 10^{-6}$. Once the maximal generation L is fixed and all barriers for all generations (up to the maximal one) are shown in the picture, this picture is unchanged for all y such that $y < y^*$. According to our definition, these barriers are normalized in such a way that the height of the largest barrier is equal to 1.

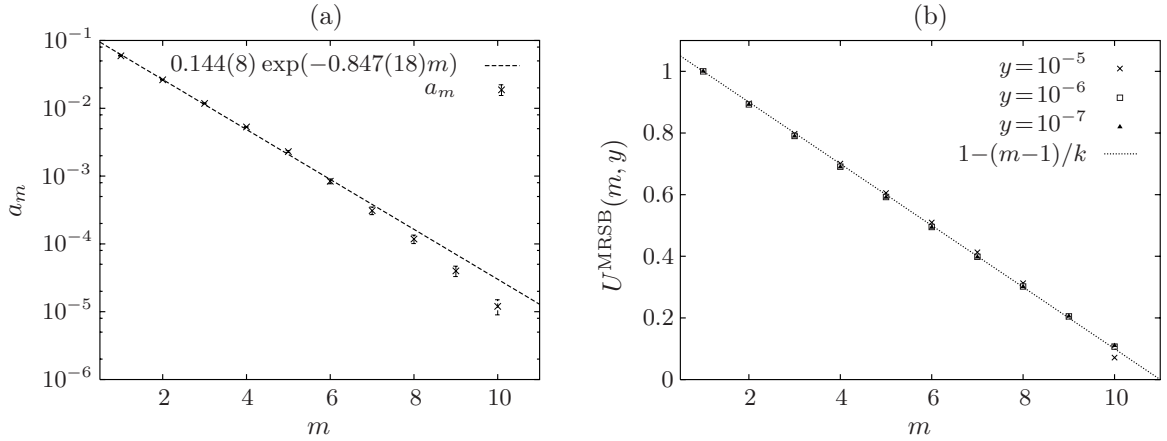

Fig. 6. (a) Approximation of the coefficient a_m. (b) Ultrametric barriers $U^{\rm MRSB}(m, y) = \frac{1}{c(y)\,L} \times \ln \frac{h(m,y)}{h(1,y)}$

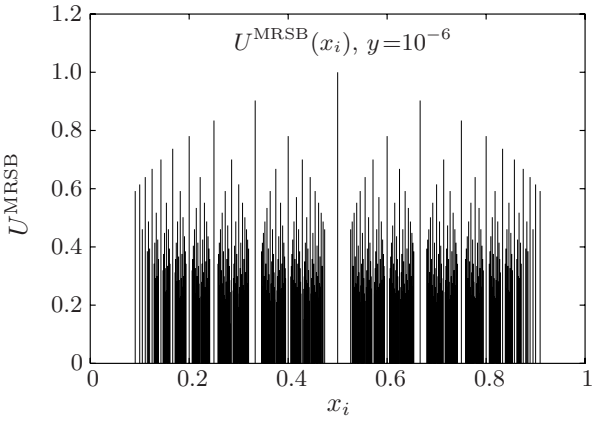

Fig. 7. Ultrametric barriers $U^{\mathrm{MRSB}}(x_i)$ at rational points x_i for $y = 10^{-6}$

The averaged height of the barriers of the second (third, forth, etc.) generation is equal to 0.9 (0.8, 0.7, etc.) (compare with (19)). Let us repeat that, in Fig. 7, we have displayed the barriers corresponding to generations m up to $m = L$. We can easily relax this condition and work with the set of *all* possible barriers up to some fixed minimal value $y_{\min}$ without paying attention to how many generations are counted.

5. DESCRIPTION OF DYNAMICAL MODELS

Our aim is to investigate numerically the probability distribution of a random walk on the boundary of an ultrametric tree. This problem was the subject of the original work [18], where the dynamics in the ultrametric space was considered in the framework of the discrete model of jumps on the boundary of a 3-branching Cayley tree. The first application of p-adic analysis to the computation of the probability distribution of diffusion at the boundary of an ultrametric tree was successfully realized in [9].

Below, we reconsider the diffusion problem in the continuous metric space, where the ultrametric organization of barriers is due to the modular structure of the Dedekind function. The advantages of such consideration are discussed in the conclusion. Let us specify the models under consideration.

I. The standard RSB model. In this model, we consider random jumps at the boundary of a 3-branching Cayley tree (see Fig. 3). The transition probabilities between the Cayley tree vertices are encoded in the matrix (14). As explained above, we fix the total number of generations L and set the highest barrier (in the first generation) always equal to 1. Then, the heights of the barriers of generation m are given by (19), while the height of the smallest barriers in the generation L is equal to $\frac{1}{L}$. Increasing the number of generations L, we increase the resolution of our model without changing the value of the maximal barrier. We use this problem of diffusion on the boundary of a standard 3-branching Cayley tree as a testing area for diffusion in the continuous treelike ultrametric space.

Let $P_N(k, k_0)$ be the partition function of the random walk starting at the point k_0 and ending after N steps at the point k, where k labels the vertices of the Lth generation of the Cayley tree and both points k_0 and k belong to the Lth generation of the tree. The corresponding diffusion is governed by the recursion relation

$$\begin{cases} P^{\mathrm{RSB}}_{N+1}(k) = \displaystyle\sum_{k'=1}^{2^L} Q^{\mathrm{RSB}}(k,k')P^{\mathrm{RSB}}_N(k'), \\ P^{\mathrm{RSB}}_{N=0}(k) = \delta_{k,k_0}, \end{cases} \tag{26}$$

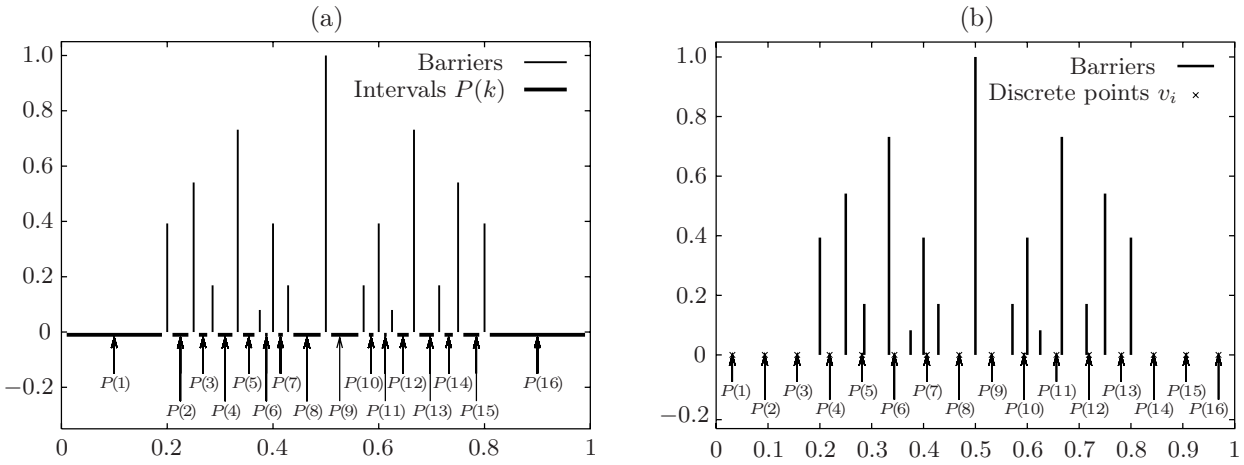

Fig. 8. Location of barriers up to four generations; (a) model I: the values v_i correspond to the intervals between maxima; (b) model II: the values v_i correspond to discrete points

where $Q^{\mathrm{RSB}}(k,k')$ is a $2^L \times 2^L$ matrix whose elements are the Boltzmann weights associated with jumps from some point k_1 to a point k_2 ($k_1, k_2 \in [1, 2^L]$) at the boundary of the 3-branching Cayley tree cut at the generation L. In order to take into account the ultrametricity of the Cayley tree, the matrix $Q^{\mathrm{RSB}}(k,k')$ should have the RSB structure and hence should coincide with the matrix $\mathbf{Q}$ in (14).

II. The quasi-continuous MRSB model. This model is defined as follows. We fix the maximal generation L and consider the heights of the potential U^{MRSB} (see (25)) corresponding to generations less than or equal to L. For example, in Fig. 8a, we plot $15 = 2^L - 1 = n$ barriers up to the generation $L = 4$. The rational points x_i, $i = 1, 2, \ldots, 15$, split the interval $[0,1]$ into 16 subintervals $[x_{i-1}, x_i]$ (including the subintervals $[0, x_1]$ and $[x_{15}, 1]$). A random walker can jump from one interval to any other. Let us enumerate the intervals by the variable $k = 1, 2, 3, \ldots, 16$. So, $k = 1$ denotes the interval $[0, x_1]$, $k = 2$ is the interval $[x_1, x_2]$, etc. Let $U^{\mathrm{MRSB}}(k,k')$ be the maximal barrier between the intervals k and k' defined by (25). By construction, $U^{\mathrm{MRSB}}(k,k) = 0$. According to our rules, if $x \in [x_{k-1}, x_k]$ and $x' \in [x_{k'-1}, x_{k'}]$, then $U^{\mathrm{MRSB}}(x,x') = U^{\mathrm{MRSB}}(k,k')$. Thus, we can write a recursive relation for the continuous distribution function $W_N(x)$. This function is defined for $x \in \mathbb{R}$ ($0 \le x \le 1$), where N enumerates the time moments. In this quasi-continuous MRSB case, we claim that the master equation has the following form instead of equation (26):

$$\begin{cases} W_{N+1}(x) = \displaystyle\int_0^1 dx'\, e^{-\beta U^{\mathrm{MRSB}}(x,x')}\, W_N(x'), \\ W_{N=0}(x) = \delta_{x,x_0}. \end{cases} \tag{27}$$

We can transform (27) making it more similar to (26). Namely, define $P_N^{\mathrm{MRSB}}(k)$, the probability that the walker belongs to the kth interval after the Nth jump (time step), as follows:

$$P_N^{\mathrm{MRSB}}(k) = \int_{x_{k-1}}^{x_k} W_N(x)\, dx. \tag{28}$$

The normalization of the probability defines the sum over all intervals $\sum_{k=1}^{n} P_N^{\mathrm{MRSB}}(k) = \int_0^1 W_N(x)\, dx = 1$. Integrating (27) over the interval $[0,1]$ and replacing the integrals with respect

to dx and dx' by sums over k and k', we get

$$\sum_{k=1}^{n} P_{N+1}^{\mathrm{MRSB}}(k) = \int_0^1 W_{N+1}(x)\,dx = \int_0^1\int_0^1 e^{-\beta U^{\mathrm{MRSB}}(x,x')}\, W_N(x')\,dx'\,dx$$

$$= \sum_{k=1}^{n}\sum_{k'=1}^{n} \int_{x_{k-1}}^{x_k}\int_{x'_{k'-1}}^{x'_{k'}} e^{-\beta U^{\mathrm{MRSB}}(x,x')} W_N^{\mathrm{MRSB}}(x')\,dx'\,dx \tag{29}$$

$$= \sum_{k=1}^{n}\sum_{k'=1}^{n} l_k e^{-\beta U^{\mathrm{MRSB}}(k,k')} P_N^{\mathrm{MRSB}}(k'),$$

where l_k is the length of the kth interval, $l_k = \int_{x_{k-1}}^{x_k} dx = x_k - x_{k-1}$. Here, we have used (28) to express $P_{N+1}^{\mathrm{MRSB}}(k)$ and $P_N^{\mathrm{MRSB}}(k')$ via $W_{N+1}^{\mathrm{MRSB}}(x)$ and $W_N^{\mathrm{MRSB}}(x')$. Now, we can separate equations for different k and write

$$P_{N+1}^{\mathrm{MRSB}}(k) = \sum_{k'=1}^{n} Q(k,k') P_N^{\mathrm{MRSB}}(k'), \tag{30}$$

where

$$Q(k,k') = l_k e^{-\beta U^{\mathrm{MRSB}}(k,k')} \tag{31}$$

is the probability for the walker to jump from the interval k' to the interval k. This probability is the product of the measure of the appropriate interval l_k and the Boltzmann weight $e^{-\beta U^{\mathrm{MRSB}}(k,k')}$. Define a vector $\mathbf{P}_N^{\mathrm{MRSB}}$ whose elements $P_N^{\mathrm{MRSB}}(k)$ are the probabilities for the walker to reach the interval k after the Nth jump. The vector $\mathbf{P}_0^{\mathrm{MRSB}}$ is the initial probability distribution on the intervals. Introduce a matrix $\mathbf{Q}$ with the elements $Q(k,k')$ and a matrix $\mathbf{U}^{\mathrm{MRSB}}$ with the elements $U^{\mathrm{MRSB}}(k,k')$. The elements of these two matrices are connected by relation (31). The probability for the walker to reach the interval k at the time moment N is the kth element of the vector $\mathbf{P}_N^{\mathrm{MRSB}}$:

$$\mathbf{P}_N^{\mathrm{MRSB}} = \mathbf{Q}^N \mathbf{P}_0^{\mathrm{MRSB}}. \tag{32}$$

Recall that the barrier $U^{\mathrm{MRSB}}(k,k')$ between the points k and k' is the highest barrier on the interval $[k,k']$. Such barriers are located at the rational points $\{k_m\}$. This defines the ultrametric structure of the matrix $\mathbf{U}^{\mathrm{MRSB}}$ and, therefore, of $\mathbf{Q}$. By construction, the matrix $\mathbf{U}^{\mathrm{MRSB}}$ reflects the ultrametric hierarchy of barriers appearing in the standard RSB matrix (see (14)). For example, the structure of the modular MRSB matrix $\mathbf{U}^{\mathrm{MRSB}}$ that defines the heights of barriers between all the intervals along the x-axis for $L = 8$ is displayed below:

$$\mathbf{U}^{\mathrm{MRSB}} = \left(\begin{array}{cc|cc|cccc}
U_0 & U(\frac14) & U(\frac13) & U(\frac13) & U(\frac12) & U(\frac12) & U(\frac12) & U(\frac12) \\
U(\frac14) & U_0 & U(\frac13) & U(\frac13) & U(\frac12) & U(\frac12) & U(\frac12) & U(\frac12) \\
\hline
U(\frac13) & U(\frac13) & U_0 & U(\frac25) & U(\frac12) & U(\frac12) & U(\frac12) & U(\frac12) \\
U(\frac13) & U(\frac13) & U(\frac25) & U_0 & U(\frac12) & U(\frac12) & U(\frac12) & U(\frac12) \\
\hline
U(\frac12) & U(\frac12) & U(\frac12) & U(\frac12) & U_0 & U(\frac35) & U(\frac23) & U(\frac23) \\
U(\frac12) & U(\frac12) & U(\frac12) & U(\frac12) & U(\frac35) & U_0 & U(\frac23) & U(\frac23) \\
\hline
U(\frac12) & U(\frac12) & U(\frac12) & U(\frac12) & U(\frac23) & U(\frac23) & U_0 & U(\frac34) \\
U(\frac12) & U(\frac12) & U(\frac12) & U(\frac12) & U(\frac23) & U(\frac23) & U(\frac34) & U_0
\end{array}\right) \tag{33}$$

III. The discretized MRSB model. In this model, the location of barriers is the same as in model II, but now we split the total interval $[0,1]$ into $n=2^L$ subintervals of equal length $\frac{1}{n}$. The midpoint of the kth interval is the point $\overline{x}_k=-\frac{1}{2n}+\frac{k}{n}$. We consider the distance between intervals k and k' as the distance between the midpoints: $U^{\mathrm{III}}(k,k')=U^{\mathrm{MRSB}}(\overline{x}_k,\overline{x}_{k'})$. Namely, we consider jumps between n midpoints k ($k=1,2,\ldots,n$) with coordinates $\overline{x}_k=-\frac{1}{2n}+\frac{k}{n}$. The probability for the walker to jump from a point k' to a point k is defined by the relation

$$Q^{\mathrm{III}}(k,k')=\frac{1}{n}e^{-\beta U^{\mathrm{MRSB}}(\overline{x}_k,\overline{x}_{k'})}. \tag{34}$$

Each element $P_N^{\mathrm{III}}(k)$ of the probability vector $\mathbf{P}$ corresponds to a point. In this model, all barriers $x_i=\frac{p_i}{q_i}$ lie between the midpoints (see Fig. 8b).

Comparing models II and III, it is easy to understand that the number n of points $\overline{x}_k$ in the interval $[x_k,x_{k+1}]$ between barriers plays the role of the measure of this interval.

Below, we compare the numerical solutions of models I, II, and III. To be more specific, we consider simultaneously an N-step random walk on the Cayley tree (model I) and on its continuous analogue (models II and III). First of all, we calculate the elements $[\mathbf{Q}^N](i,j)$ of the matrix $\mathbf{Q}^N$ for all three models. Then, we compute

- the probability P_0 for the walker to stay at the initial point after N random jumps,

$$P_0=\sum_{i=1}^{n}[\mathbf{Q}^N](i,i); \tag{35}$$

- the average ultrametric distance U between the initial and the final points of the N-step random walk,

$$U=\sum_{i=1}^{n}\sum_{j=1}^{n}[\mathbf{U}](i,j)[\mathbf{Q}^N](i,j), \tag{36}$$

where $[\mathbf{U}](i,j)$ is the element of the matrix $\mathbf{U}$ defining the ultrametric distances between all available points. The size of the matrices $\mathbf{U}$ and $\mathbf{Q}$ is $n=2^L$, where L is the total number of generations.

6. NUMERICAL RESULTS FOR MODELS I, II, AND III

The following three cases are studied numerically:

1. We fix the maximal generation L and the number of jumps N and plot P_0 and U as functions of the inverse temperature β (see Fig. 9) for the following numerical values of L and N: $L=10$ and $N=400$.

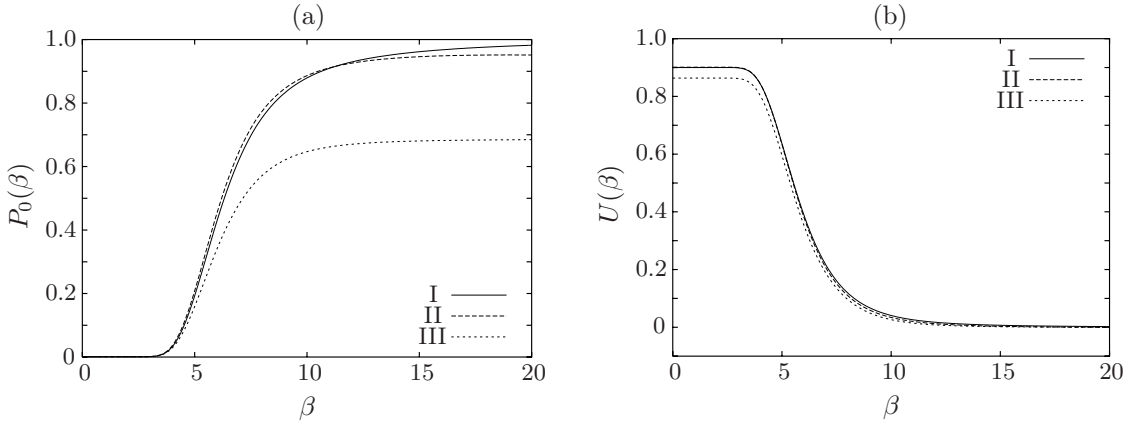

Fig. 9. (a) $P_0(\beta)$; (b) $U(\beta)$. Numerical values of the parameters are $L=10$ and $N=400$

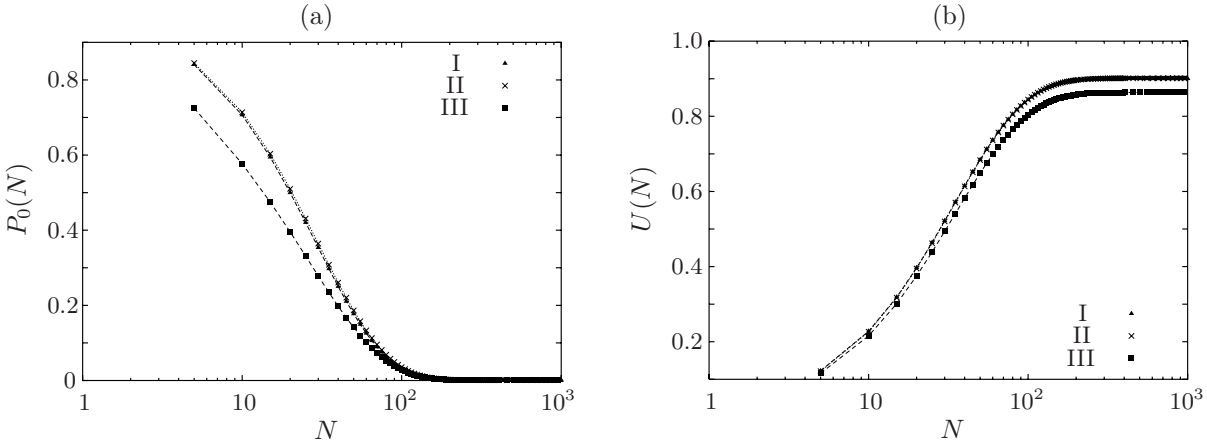

Fig. 10. (a) $P_0(N)$; (b) $U(N)$. Numerical values of the parameters are $L = 10$ and $\beta = 4$

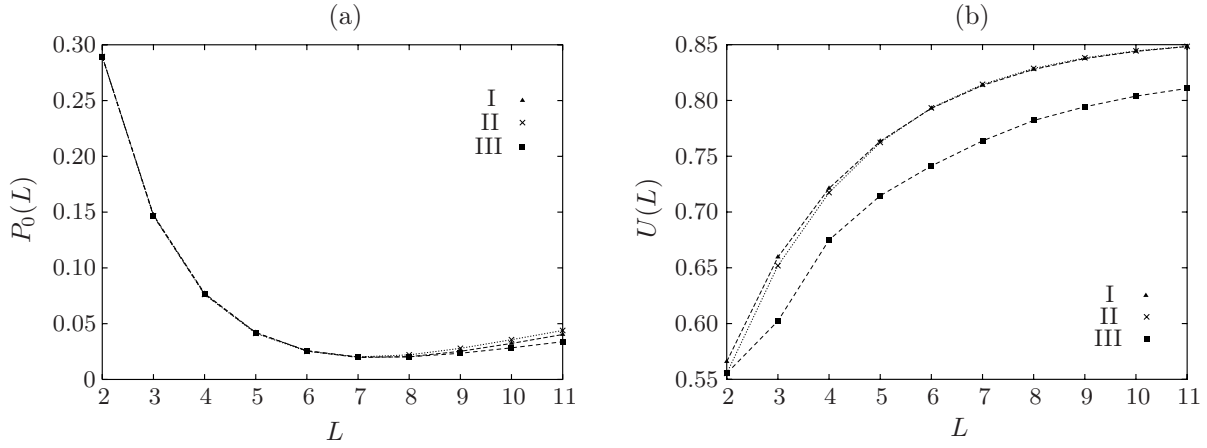

Fig. 11. (a) $P_0(L)$; (b) $U(L)$. Numerical values of the parameters are $N = 400$ and $\beta = 1$

2. We fix the maximal generation L and the inverse temperature β and plot P_0 and U as functions of the number of steps N (see Fig. 10) for the following numerical values of L and β: $L = 10$ and $\beta = 4$.

3. We fix the number of jumps N and the inverse temperature β and plot P_0 and U as functions of the maximal generation L (see Fig. 11) for the following numerical values of N and β: $N = 400$ and $\beta = 1$.

7. DISCUSSION

The numerical solution of the master equations (26) and (27) shown in Figs. 9–11 allows us to conclude that we arrive at the same results for the return probability P_0 and the mean height of the barriers U for random walks in the ultrametric spaces irrespective of the model we consider: either the ultrametric structure of the barriers is defined on the boundary of a Cayley tree (case I), or the heights of these barriers are given by a properly normalized Dedekind function (cases II and III).

Our results are obtained under the condition that the heights of the ultrametric barriers in all the models (I, II, and III) *linearly depend* on the number of Cayley tree generation. Recall that this is the only requirement imposed on the construction of our ultrametric potential (25) on the basis of the Dedekind modular function. The current choice of the potential is stipulated basically for demonstrational purposes. Namely, we have shown that it is possible to adjust the ultrametric

structure of the continuous metric space $\mathcal{H}$ to the structure of the standard Cayley tree in such a way that we can mimic the main statistical properties of the random walk at the boundary of the Cayley tree by the diffusion in $\mathcal{H}$.

The key ingredient of our construction is contained in the replacement of the RSB scheme (14) by the new MRSB scheme (33). Although the corresponding master equation (27) allows only numerical treatment, in our opinion the construction proposed offers some advantages over the RSB scheme that result from: (i) the self-duality (see (13)), and (ii) the continuity of the MRSB.

Below, we touch upon both these properties (i) and (ii) in connection with a possible simplification of the solution of the continuous analogue of the master equation (29) (see Section A below) and with speculations about the geometry of the $n \to 0$ limit (see Section B below). We clearly realize that the last subject is one of the mostly intriguing questions in the statistical physics of disordered systems, and our conjecture might be criticized from different points of view; however, we believe that our geometric construction may stimulate the readers to supplement the standard mode of thinking about replicas with some fresh geometric ideas.

A. The continuous MRSB model. Taking advantage of our construction of an ultrametric system of barriers described by the potential $U^{\mathrm{MRSB}}(x_m)$ (see (25)), we can replace the master equation (26) by its analogue based on the properties of the Dedekind function. The distribution function $W_N(x)$ is described by (27), where x_m is a rational point on the interval $[x', x]$ with the smallest denominator (there is only one such point). As we have already seen, the highest barrier $U^{\mathrm{MRSB}}(x_m)$ on the interval $[x', x]$ is located at the point x_m. The number of barriers and their heights are controlled simultaneously by the parameter y. As $y \to 0$, more and more new barriers appear. Gradually, they become higher and narrower, preserving the ultrametric structure. In this section, we are interested in the limit $y \to 0$, where the hierarchical structure of barriers is highly developed (see, for example, Fig. 7). One can simplify equation (27) by using (13). Making a substitution that maps y to $\frac{1}{y}$ in equation (27), we get

$$U^{\mathrm{MRSB}}(x_m, y, L^*) \equiv 1 + \frac{1}{cL^*(y)} \ln \frac{\ln f(x_m, y)}{\ln f(\frac{1}{2}, y)}\bigg|_{y\to 0} \simeq 1 + \frac{2}{cL^*(y)} \ln \frac{2}{q}, \tag{37}$$

where $L^*(y)$ is determined again by relation (24). Equation (37) is valid only for $\{p, q, s, r\} \in \mathbb{Z}$ such that $ps - qr = 1$ (where r may be an arbitrary integer). The point $x_m = \left\{\frac{p}{q}\right\}$ and its "dual image" $x'_m = \left\{\frac{s}{q}\right\}$ lie in the unit interval $[0, 1]$. Substituting (37) into (27), we have

$$\begin{cases} W_{N+1}(x) = \displaystyle\int_0^1 dx'\, e^{-\beta} \left(\frac{2}{q}\right)^{2\beta/(cL^*(y))} W_N(x'), \\ W_{N=0}(x) = \delta_{x,x_0}. \end{cases} \tag{38}$$

Equation (38) has a rich number-theoretic structure. In fact, information on the position of the highest barrier in the interval $[x', x]$ is hidden in the integer q. Let us recall that the value of q should satisfy the following condition: *q is the smallest denominator of rational points $x_m = \frac{p}{q}$, $x_m \in [x', x]$*. As one can see, the value $L^*(y)$ governs the amplitude of the potential, while q controls the maximal "resolution" and, hence, the total number of barriers.

B. Speculations about a continuous number of Cayley tree generations L and the replica $n \to 0$ limit. Despite many advantages of the RSB scheme, it contains the mystery, unavoidable in the replica formalism, of the $n \to 0$ limit, where $n = 2^L$ is the number of replicas (see Fig. 12).

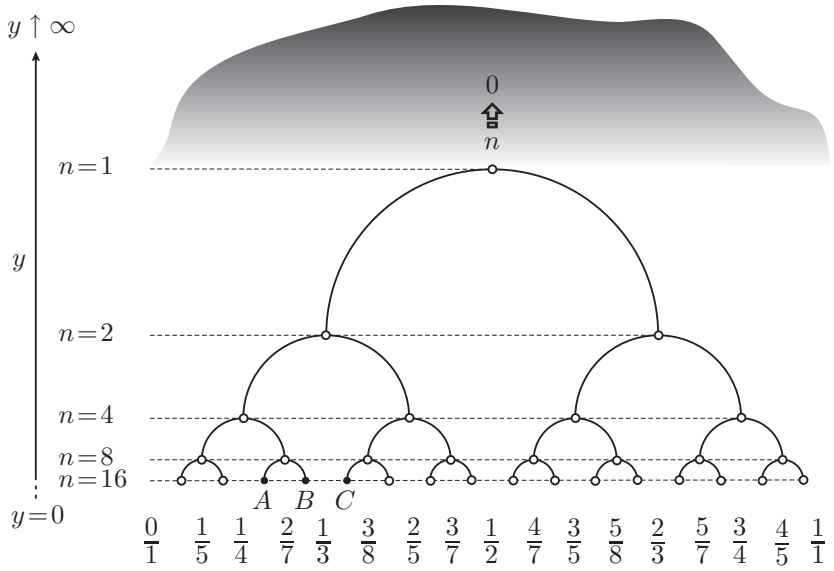

Fig. 12. The 3-branching Cayley tree. The barriers are located at rational points ordered in the Farey sequence. The replica limit $n \to 0$ is interpreted as the absence of states (vertices of the tree) when $y \to \infty$

One of the merits of our construction based on the Dedekind η function is the possibility to change continuously the number of ultrametric barriers and their heights by varying the parameter y and, hence, to change continuously the number of states n of the RSB matrix. Let us recall that a standard 3-branching Cayley tree, being isometrically embedded into the space $\mathcal{H} = \{z \mid \operatorname{Im} z > 0\}$, becomes a "continuous" structure: one can define the smoothed neighborhood of maxima of the function $f(z)$ in the half-plane $y = \operatorname{Im} z > 0$ (see Fig. 1). For instance, our construction allows us to increase continuously the number of states n from, say, $n = 1$ to $n = 2$ by appropriately varying the parameter y in the interval $[y_{n=1}, y_{n=2}]$, where $y_{n=1} = \frac{\sqrt{3}}{6}$ and $y_{n=2} = \frac{\sqrt{3}}{14}$.

Our geometric construction based on the isometric embedding of a Cayley tree into the complex plane also permits us to consider the opposite limit, the case when n is formally less than 1. This case means the absence of any states in the RSB matrix ($n = 0$). As one can see from Figs. 1 and 2, the function $f(z)$ does not have local maxima above the value $y \equiv \operatorname{Im} z > \frac{\sqrt{3}}{2}$ any longer. As soon as we have identified the local maxima of the function $f(z)$ with the vertices (states) of the Cayley tree, we conclude that the absence of any states of the RSB matrix means the absence of local maxima of the function $f(z)$. Thus, the limit $n \to 0$ is interpreted as $y \to \infty$. This claim is based on the behavior of the function $f(z)$ in the upper half-plane. The correspondence of the limits $n \to 0$ and $y \to \infty$ is schematically illustrated in Fig. 12. The geometrical interpretation of the number of replica states in the region $0 < n < 1$ makes the physical statement about the "analytic continuation $n \to 0$" more formal. Actually, let us recall the definition of the hyperbolic distance $\mathcal{L}$ in $\mathcal{H}(z \mid \operatorname{Im} z > 0)$ between two points $z_0 = (x_0, y_0)$ and $z = (x, y)$:

$$\cosh \mathcal{L} = 1 + \frac{(x - x_0)^2 + (y - y_0)^2}{y_0 y}. \tag{39}$$

As we have seen, the hyperbolic distance $\mathcal{L}$ is a continuous analogue of the number of Cayley tree generations L, which permits us to define the number of replica states n as

$$n = e^{\text{const} \cdot \mathcal{L}}. \tag{40}$$

As $y \to 0$, we can replace $\cosh \mathcal{L}$ with the leading exponential term. In this way, we arrive at the standard relation $e^{\mathcal{L}} = \frac{2y}{y_0}$. Hence,

$$\frac{e^{\mathcal{L}}}{2} + \cancel{\frac{e^{-\mathcal{L}}}{2}} = \frac{(x-x_0)^2 + y_0^2}{y_0 y}. \tag{41}$$

Neglecting the second term on the left-hand side of (41), we get

$$\mathcal{L} = -\ln y + c_1, \qquad y \to 0,$$

where $c_1 = \ln \frac{2((x-x_0)^2+y_0^2)}{y_0}$.

However, if $y \to \infty$, equation (39) gives

$$\cancel{\frac{e^{\mathcal{L}}}{2}} + \frac{e^{-\mathcal{L}}}{2} = \frac{y}{y_0}, \tag{42}$$

where, according to the physical condition $n \to 0$ and equation (40), we have to take another branch of the function $\operatorname{arccosh}(\ldots)$, which corresponds to the negative values of $\mathcal{L}$. This leads to the following definition of $\mathcal{L}$:

$$\mathcal{L} = -\ln y + c_2, \qquad y \to \infty, \tag{43}$$

where $c_2 = \ln \frac{y_0}{2}$. As $y \to \infty$, the hyperbolic distance $\mathcal{L}$ defined according to (43) tends to $-\infty$. Equation (43) is consistent with the definition (40) of the number of replicas n in the region $0 < n < 1$.

It would be very desirable to check how our conjecture works in the models possessing the RSB symmetry of the order parameter. We expect that our construction may be useful for investigating the aging phenomena considered from the point of view of diffusion in the whole ultrametric space $\mathcal{H}(z \mid \operatorname{Im} z > 0)$.

Acknowledgments. The main part of this work was accomplished thanks to the hospitality of the laboratory LIFR-MIIP (CNRS, France and Independent University, Moscow); O. Vasilyev thanks the laboratory LPTMS (Université Paris Sud, Orsay) for the hearty welcome.

REFERENCES

1. *Rammal R., Toulouse G., Virasoro M.A.* Ultrametricity for physicists // Rev. Mod. Phys. 1986. V. 58. P. 765–788.
2. *Brekke L., Freund P.G.O.* p-Adic numbers in physics // Phys. Rept. 1993. V. 233. P. 1–66.
3. *Владимиров В.С., Волович И.В., Зеленов Е.И.* p-Адический анализ и математическая физика. М.: Наука, 1994.
4. *Mezard M., Parisi G., Virasoro M.* Spin glass theory and beyond. Singapore: World Sci., 1987.
5. *Parisi G.* Infinite number of order parameters for spin-glasses // Phys. Rev. Lett. 1979. V. 43. P. 1754–1756.
6. *Parisi G.* A sequence of approximated solutions to the S-K model for spin glasses // J. Phys. A: Math. and Gen. 1980. V. 13. P. L115–L121.
7. *Parisi G.* The order parameter for spin glasses: a function on the interval 0–1 // J. Phys. A: Math. and Gen. 1980. V. 13. P. 1101–1112.
8. *Parisi G.* Magnetic properties of spin glasses in a new mean field theory // J. Phys. A: Math. and Gen. 1980. V. 13. P. 1887–1895.
9. *Avetisov V.A., Bikulov A.H., Kozyrev S.V.* Application of p-adic analysis to models of breaking of replica symmetry // J. Phys. A: Math. and Gen. 1999. V. 32. P. 8785–8791.
10. *Parisi G., Sourlas N.* p-Adic numbers and replica symmetry breaking // Eur. Phys. J. B. 2000. V. 14. P. 535–542.
11. *Avetisov V.A., Bikulov A.H., Kozyrev S.V., Osipov V.A.* p-Adic models of ultrametric diffusion constrained by hierarchical energy landscapes // J. Phys. A: Math. and Gen. 2002. V. 35. P. 177–189.

12. *Avetisov V.A., Bikulov A.Kh., Osipov V.A.* p-Adic description of characteristic relaxation in complex systems // J. Phys. A: Math. and Gen. 2003. V. 36. P. 4239–4246.
13. *Carlucci D.M., De Dominicis C.* On the replica Fourier transform // C. r. Acad. sci. Paris. Ser. IIB: Mech. Phys. Chim. Astr. 1997. V. 325. P. 527–530.
14. *De Dominicis C., Carlucci D.M., Temesvari T.* Replica Fourier transforms on ultrametric trees, and block-diagonalizing multi-replica matrices // J. phys. I (France). 1997. V. 7. P. 105–115.
15. *Terras A.* Harmonic analysis on symmetric spaces and applications. New York: Springer, 1985. V. 1.
16. *Chandrasekharan K.* Elliptic functions. Berlin: Springer, 1985.
17. *Di Francesco P., Senechal D., Mathieu P.* Conformal field theory. Berlin: Springer, 1996.
18. *Ogielski A.T., Stein D.L.* Dynamics on ultrametric spaces // Phys. Rev. Lett. 1985. V. 55. P. 1634–1637.
19. *Bachas C.P., Huberman B.A.* Complexity and ultradiffusion // J. Phys. A: Math. and Gen. 1987. V. 20. P. 4995–5014.
20. *Magnus W.* Noneuclidean tesselations and their groups. London: Acad. Press, 1974.
21. *Beardon A.F.* The geometry of discrete groups. Berlin: Springer, 1983.